Article

Cancer Cell

A LIN28B-RAN-AURKA Signaling Network Promotes Neuroblastoma Tumorigenesis

Graphical Abstract

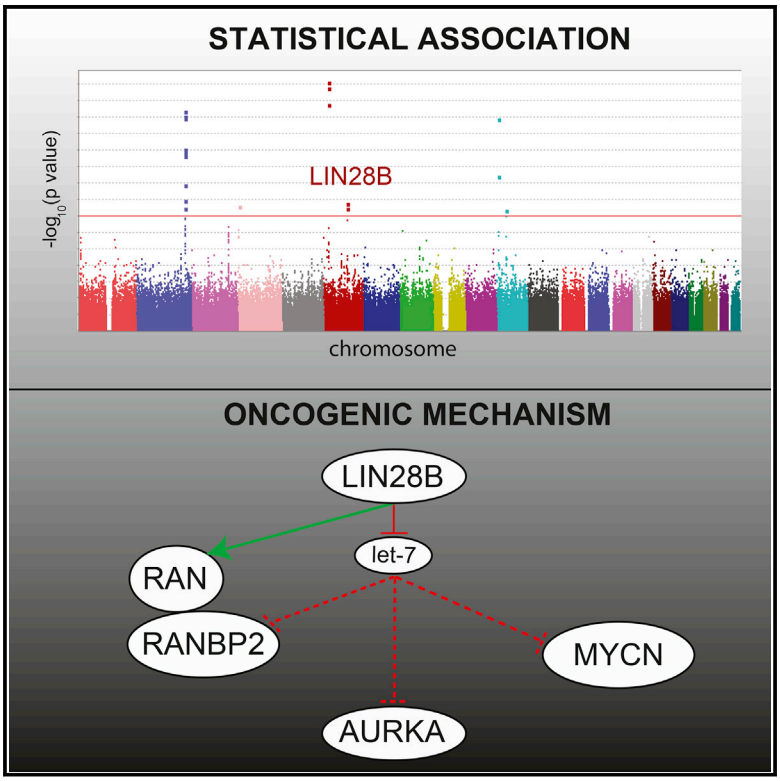

Highlights

- LIN28B and regional gain of chromosome 12q24 mediate RAN oncogene overexpression
- RAN promotes cell proliferation in neuroblastoma
- LIN28B promotes RAN levels by binding *RAN* mRNA and via RAN binding protein 2
- LIN28B promotes Aurora kinase A expression in a let-7-dependent manner

Authors

Robert W. Schnepp, Priya Khurana, Edward F. Attiyeh, ..., Anil K. Rustgi, John M. Maris, Sharon J. Diskin

Correspondence

maris@email.chop.edu (J.M.M.), diskin@email.chop.edu (S.J.D.)

In Brief

Extending from prior identification of LIN28B as an oncogenic driver in high-risk neuroblastoma, Schnepp et al. show that LIN28B regulates the RAN level directly by mRNA binding and indirectly via let-7-regulated RANBP2. LIN28B and RAN signaling converge on Aurora kinase A, suggesting therapeutic potential.

Schnepp et al., 2015, Cancer Cell *28*, 599–609
November 9, 2015 ©2015 Elsevier Inc.
http://dx.doi.org/10.1016/j.ccell.2015.09.012

Cancer Cell
Article

A LIN28B-RAN-AURKA Signaling Network Promotes Neuroblastoma Tumorigenesis

Robert W. Schnepp,[1] Priya Khurana,[1] Edward F. Attiyeh,[1,2] Pichai Raman,[1,3] Sara E. Chodosh,[1] Derek A. Oldridge,[1] Maria E. Gagliardi,[1] Karina L. Conkrite,[1] Shahab Asgharzadeh,[4] Robert C. Seeger,[4] Blair B. Madison,[5] Anil K. Rustgi,[6,7,8,9] John M. Maris,[1,2,10,11,*] and Sharon J. Diskin[1,2,10,11,*]
[1]Division of Oncology and Center for Childhood Cancer Research, Children's Hospital of Philadelphia, Philadelphia, PA 19104, USA
[2]Department of Pediatrics, Perelman School of Medicine, University of Pennsylvania, Philadelphia, PA 19104, USA
[3]Department of Biomedical and Health Informatics, The Children's Hospital of Philadelphia, Philadelphia, PA 19104, USA
[4]Division of Hematology, Oncology, and Blood and Marrow Transplantation, Department of Pediatrics, Children's Hospital Los Angeles, Los Angeles, CA 90027, USA
[5]Division of Gastroenterology, Washington University School of Medicine in St. Louis, St. Louis, MO 63110, USA
[6]Abramson Cancer Center, Perelman School of Medicine, University of Pennsylvania, Philadelphia, PA 19104, USA
[7]Division of Gastroenterology, Perelman School of Medicine, University of Pennsylvania, Philadelphia, PA 19104, USA
[8]Department of Medicine, Perelman School of Medicine, University of Pennsylvania, Philadelphia, PA 19104, USA
[9]Department of Genetics, Perelman School of Medicine, University of Pennsylvania, Philadelphia, PA 19104, USA
[10]Abramson Family Cancer Research Institute, Perelman School of Medicine at University of Pennsylvania, Philadelphia, PA 19104, USA
[11]Co-senior author
*Correspondence: maris@email.chop.edu (J.M.M.), diskin@email.chop.edu (S.J.D.)
http://dx.doi.org/10.1016/j.ccell.2015.09.012

SUMMARY

A more complete understanding of aberrant oncogenic signaling in neuroblastoma, a malignancy of the developing sympathetic nervous system, is paramount to improving patient outcomes. Recently, we identified *LIN28B* as an oncogenic driver in high-risk neuroblastoma. Here, we identify the oncogene *RAN* as a LIN28B target and show regional gain of chromosome 12q24 as an additional somatic alteration resulting in increased *RAN* expression. We show that LIN28B influences RAN expression by promoting RAN Binding Protein 2 expression and by directly binding *RAN* mRNA. Further, we demonstrate a convergence of LIN28B and RAN signaling on Aurora kinase A activity. Collectively, these findings demonstrate that LIN28B-RAN-AURKA signaling drives neuroblastoma oncogenesis, suggesting that this pathway may be amenable to therapeutic targeting.

INTRODUCTION

Defining optimal therapy for patients with neuroblastoma, a pediatric malignancy of the developing sympathetic nervous system, continues to present a significant challenge. Although patients with high-risk disease undergo an intense multimodal treatment regimen, cure rates remain below 50% and survivors are burdened with significant long-term morbidities (Maris, 2010). The advent of high-throughput genomic sequencing has defined the landscape of somatically acquired mutations in neuroblastoma (Cheung et al., 2012; Molenaar et al., 2012b; Sausen et al., 2013; Pugh et al., 2013), uncovering oncogenic drivers that might provide opportunities for therapeutic targeting. While *MYCN*, *ALK*, *ATRX*, *PTPN11*, *ARID1A*, and *ARID1B* are somatically altered in neuroblastoma, the relatively low frequency of such alterations, ranging from 1.7% to 11% (Cheung et al., 2012; Molenaar et al., 2012b; Sausen et al., 2013; Pugh et al., 2013; Bresler et al., 2014), challenge strategies that rely upon

Significance

Children diagnosed with high-risk neuroblastoma are treated with intense multimodal therapies, yet cure rates remain well below 50%, underscoring the need for more effective therapies. Recurrent somatic mutations are relatively infrequent in neuroblastoma, presenting challenges to therapeutic strategies that rely on targeting such oncogenic drivers. However, germline variation in tumor suppressors or oncogenes such as LIN28B also contributes to neuroblastoma initiation and maintenance, but the mechanisms for these associations are largely not defined. Here, we show that LIN28B coordinates the expression of the oncogenes RAN and AURKA in neuroblastoma, influencing these oncogenes in both let-7-dependent and -independent manners. Our findings define the aberrant signaling driven by LIN28B in neuroblastoma and provide a necessary foundation for developing better treatment strategies.

drugging frequently altered oncogenic drivers. Genome-wide association studies (GWAS) have highlighted the importance of germline variation in both disease susceptibility and in orchestrating the tumor phenotype, unveiling *BARD1* (Capasso et al., 2009; Bosse et al., 2012), *LMO1* (Wang et al., 2011) and, most recently, *LIN28B* (Diskin et al., 2012), as predisposition genes and oncogenic drivers in neuroblastoma subsets. *LIN28B* is of particular interest, as we (Diskin et al., 2012) and others (Molenaar et al., 2012a) have shown that it is involved in disease initiation, is highly expressed in neuroblastoma, and promotes *MYCN* expression.

LIN28B and its paralog LIN28A are RNA binding proteins that mediate diverse biological functions. The LIN28 family regulates mammalian stem cell self-renewal and LIN28A, in combination with NANOG, OCT4, and SOX2, can reprogram human somatic cells to pluripotent stem cells (Yu et al., 2007). LIN28A and LIN28B play crucial roles in glucose metabolism, positively regulating the insulin-PI3K-mTOR pathway (Zhu et al., 2011). LIN28A promotes tissue repair, mediated in part by binding and positively regulating genes involved in glycolysis and oxidative phosphorylation (Shyh-Chang et al., 2013). LIN28 participates in these key biological processes in part by blocking the maturation of the tumor suppressor microRNA let-7 family (Viswanathan et al., 2008; Piskounova et al., 2011). In humans, there are 11 closely related let-7 family members that mediate crucial functions, such as inhibiting cell proliferation, promoting differentiation (Boyerinas et al., 2010), and repressing expression of *KRAS* (Esquela-Kerscher et al., 2008), *MYC* (Sampson et al., 2007), and *HMGA2* (Park et al., 2007). Additionally, LIN28B binds mRNAs directly, suggesting additional mechanisms by which it influences gene expression (Peng et al., 2011; Cho et al., 2012; Wilbert et al., 2012; Hafner et al., 2013; Madison et al., 2013). Consistent with its oncogenic role, *LIN28B* is highly expressed in cancers of the colon (King et al., 2011a, 2011b) and ovary (Helland et al., 2011), Wilms tumor, germ cell tumors (Viswanathan et al., 2009), and hepatocellular carcinomas (Wang et al., 2010). Mice overexpressing *LIN28B* in the sympathoadrenal lineage develop neuroblastoma (Molenaar et al., 2012a), mice with intestine targeted *LIN28B* expression develop colonic adenocarcinomas (Madison et al., 2013), mice overexpressing *LIN28B* in the embryonic kidney develop Wilms tumor (Urbach et al., 2014), and mice overexpressing *LIN28B* in hepatic precursors develop hepatoblastomas and hepatocellular carcinoma (Nguyen et al., 2014). Collectively, these studies highlight the role of LIN28B in oncogenesis, suggesting LIN28B influences multiple oncogenic signaling networks in diverse cellular contexts. Our prior work identified germline variation at *LIN28B* as cancer predisposing and demonstrated yet another potential mechanism influencing LIN28B expression in normal development and cancer (Diskin et al., 2012). Here we sought to determine the mechanisms by which LIN28B influences neuroblastoma tumorigenesis, ultimately seeking to define opportunities for therapeutic manipulation.

RESULTS

LIN28B Expression and Chromosome 12q Gain Are Associated with *RAN* Oncogene Expression

To define oncogenic signaling networks strongly influenced by LIN28B in neuroblastoma, we performed mRNA expression profiling of 250 primary diagnostic neuroblastoma tumors obtained via the Children's Oncology Group (COG) and the Therapeutically Applicable Research to Generate Effective Treatments project (TARGET; https://ocg.cancer.gov/programs/target). We focused on high-risk neuroblastoma, considering *MYCN* amplified (n = 68) and non-amplified (n = 182) tumors separately, and defined two cohorts at the extremes of *LIN28B* expression (n = 20 per cohort; 10 highest, 10 lowest). Utilizing significance analysis of microarray (SAM) analyses, we assessed differential expression of 17,574 transcripts and utilized the Ingenuity Pathway Analysis (IPA; http://www.ingenuity.com) to assess association with canonical molecular pathways. This analysis showed several biologically relevant gene sets significantly associated with *LIN28B* expression, including several DNA damage response and cell cycle regulation gene sets, as well as RAN signaling (Tables S1 and S2). These results are consistent with multiple previous investigations that utilized high-throughput sequencing approaches to identify LIN28-bound mRNAs and that demonstrated a key role for the LIN28 family in cell cycle regulation (Peng et al., 2011; Cho et al., 2012; Wilbert et al., 2012; Hafner et al., 2013; Madison et al., 2013), as well as with studies linking LIN28/let-7 to DNA damage repair (Oh et al., 2010; Wang et al., 2013).

As we sought to discover uncharacterized LIN28B-influenced signaling networks, we chose to further study RAN signaling. RAN (Ras-related nuclear protein) is a small Ras-related GTPase that plays crucial roles in nuclear trafficking and cell cycle regulation (Deng et al., 2013; Clarke and Zhang, 2008) and promotes phosphorylation and activation of Aurora kinase A (AURKA; Tsai et al., 2003; Trieselmann et al., 2003), itself a therapeutic target in neuroblastoma (Maris et al., 2010; Mosse et al., 2012). Moreover, RAN is overexpressed in multiple malignancies including breast, lung, prostate, and colon cancer (Xia et al., 2008). Whereas KRAS is a known let-7 target (Esquela-Kerscher et al., 2008), the role of RAN in aberrant oncogenic signaling and its relationship to LIN28B had not been previously defined.

Because *LIN28B* expression is high in *MYCN* amplified neuroblastoma (Diskin et al., 2012; Molenaar et al., 2012a), we first focused on IPA results in the *MYCN* amplified cohort and observed RAN signaling as one of the top associated canonical pathways ($p = 6.9 \times 10^{-6}$; rank: 10/231 pathways tested). Multiple pathway members exhibited significantly increased expression in high *LIN28B*-expressing tumors at a SAM q-value of 0.01, including RAN itself (Table S3). Evaluation of IPA results for the *MYCN* non-amplified cohort confirmed an association of *LIN28B* expression and RAN signaling ($p = 0.0017$; rank 16/200 pathways tested; Tables S2 and S4). We observed that *LIN28B* and *RAN* expression are highly correlated in neuroblastoma, in the *MYCN*-amplified subset of cases (Figure 1A) and more modestly in the non *MYCN*-amplified subset of cases (Figure 1B). We validated these findings in two additional neuroblastoma datasets (Valentijn et al., 2012; Oberthuer et al., 2010; Figures S1A and S1B).

RAN is located at chromosome 12q24, a region that we (Wang et al., 2011; Figures S1C–S1E) and others (Wolf et al., 2010) have shown to harbor recurrent DNA copy number gain in neuroblastoma. Here, we measured DNA copy number alterations using single nucleotide polymorphism (SNP) arrays in 373 high-risk neuroblastoma primary tumors and confirmed 12q24 as a region

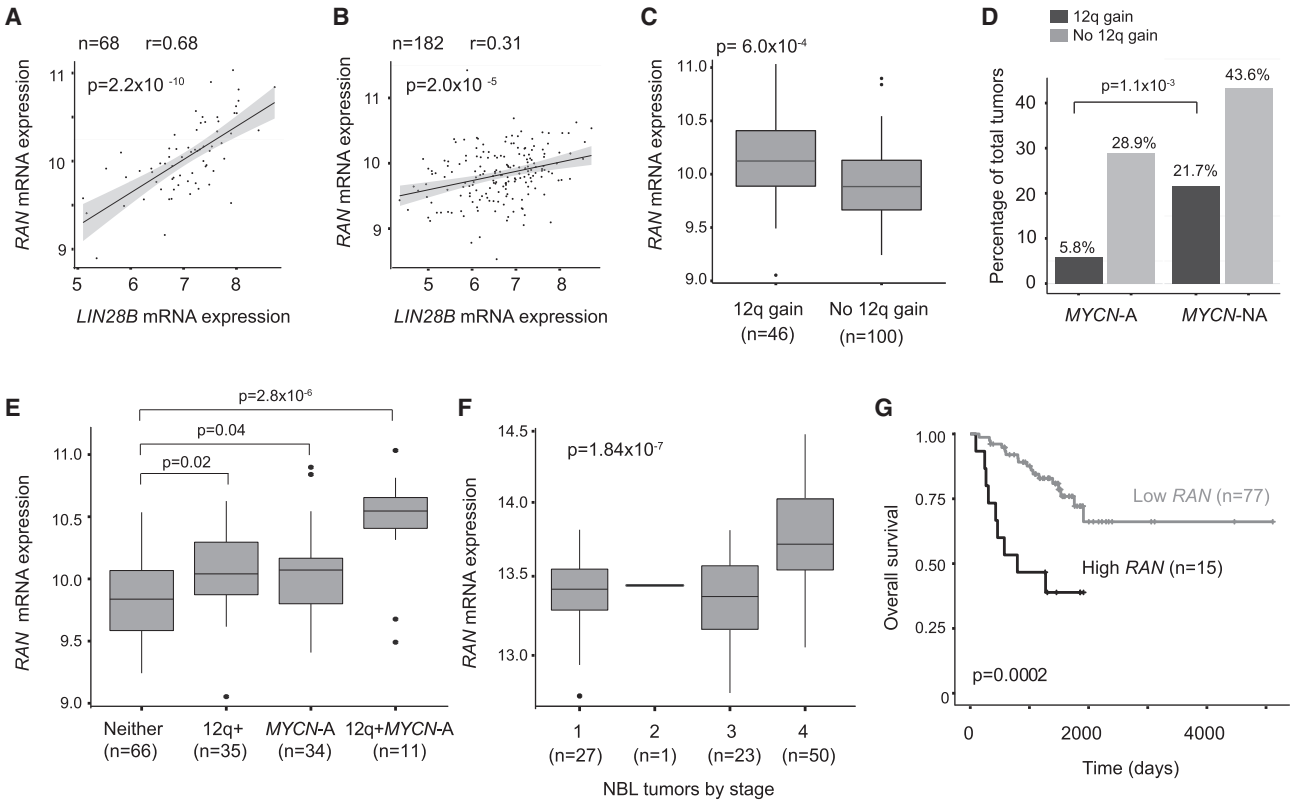

Figure 1. *LIN28B* Expression and Chromosome 12q Gain Are Positively Correlated with the Expression of the *RAN* Oncogene

(A and B) Correlation between *LIN28B* and *RAN* expression in 68 high-risk, *MYCN*-amplified (A) and 182 *MYCN*-non-amplified primary neuroblastomas (B).

(C) *RAN* mRNA expression in neuroblastoma tumors with and without 12q gain.

(D) Neuroblastomas with and without 12q gain in the context of *MYCN*-amplified (*MYCN*-A) and *MYCN*-non-amplified (*MYCN*-NA) tumors. Data analyzed using Pearson's Chi-square test, with a degree of freedom of 1, χ^2 of 10.6039, and p = 0.0011.

(E) *RAN* mRNA expression in neuroblastoma cases with 12q gain, *MYCN* amplification, both alterations, or neither. ANOVA testing was performed, followed by a post hoc Tukey HSD test.

(F) Expression of *RAN* mRNA in primary neuroblastoma tumors, as shown for International Neuroblastoma Staging System (INSS) stages 1 through 4. The number of tumors is indicated in parentheses. Neuroblastoma datasets obtained from the TARGET Consortium.

(G) Kaplan-Meier survival analysis of patients with neuroblastoma, with individuals grouped by low and high *RAN* expression in their tumors. The p values are noted where appropriate. For box-and-whisker plots, the bottom of the boxplot corresponds to quartile 1 of the data, the inscribed line to quartile 2, and the top of the boxplot to quartile 3; lines below and above the boxplot correspond to non-outliers within the first and third quartiles. Data points beyond the lines constitute outliers.

See also Tables S1, S2, S3, S4, and S5 and Figure S1.

of significant gain (GISTIC residual q = 7.15 × 10^{-7}; Figures S1C–S1E; Beroukhim et al., 2007). All DNA copy number gains involving *RAN* were single copy; no high-level amplifications were observed (Figure S1F). Chromosome 12q24 gain was not correlated with *LIN28B* expression, but was significantly associated with increased *RAN* expression (Figure 1C) and with the *MYCN* non-amplified subset (Figure 1D). We next determined whether copy number gain and/or *MYCN* amplification increases mRNA levels of genes mapping within the 12q24 wide peak identified by GISTIC (chr12: 122,212,660–133,851,895). A total of 146 genotyped tumors overlapped with our expression array data and were divided into four distinct groups based on the presence/absence of 12q24 gain and *MYCN* amplification. A total of 79 known genes map to the 12q24 GISTIC wide peak, and we tested 67 with available probesets mapping to 12q24 for differential expression among these groups (Table S5). Both chromosome 12q24 gain and *MYCN* amplification (which is correlated with high *LIN28B* expression) were associated with higher *RAN* expression (p = 0.02 and 0.04, respectively; Figure 1E). In the relatively rare context of combined *MYCN* amplification and 12q gain (n = 11), neuroblastoma tumors showed even higher levels of *RAN* expression (Figure 1E), suggesting that LIN28B and 12q gain independently promote *RAN* expression. Indeed, only 6/67 genes tested (8.9%) showed more significant association. We next demonstrated that *RAN* expression was highly correlated with advanced stage neuroblastomas in TARGET data and in two independent neuroblastoma datasets (Valentijn et al., 2012; Oberthuer et al., 2010; Figures 1F, S1G, and S1H). Accordingly, *RAN* expression was also associated with decreased overall survival (Wang et al., 2006; Valentijn et al., 2012; Figures 1G and S1I). Although multivariate analysis did not reveal *RAN* expression to be an independent prognostic indicator of poor outcome, these data demonstrate that high *RAN* expression is a common feature of advanced

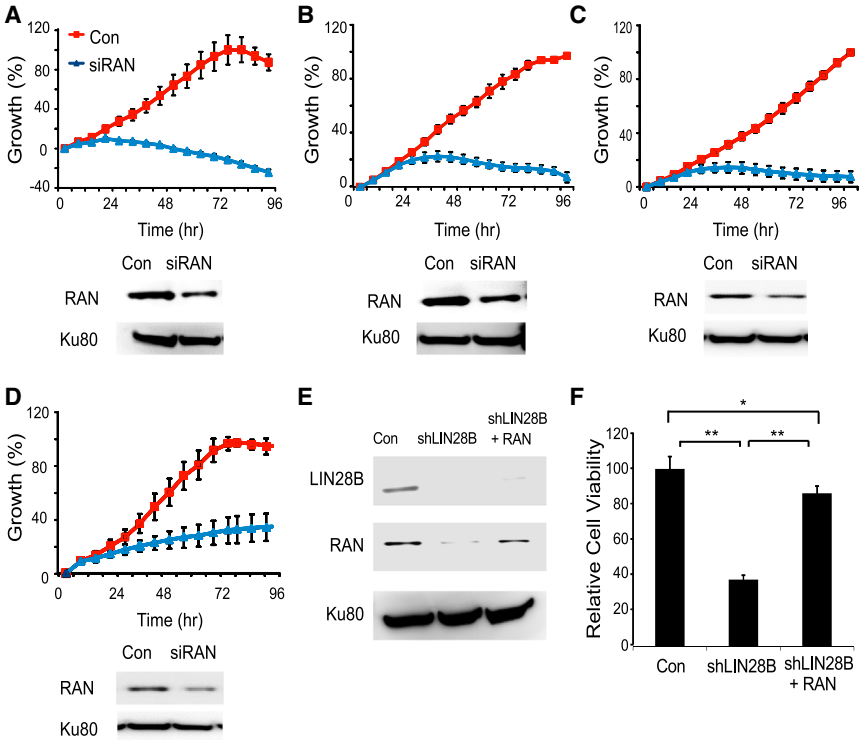

Figure 2. RAN Promotes Neuroblastoma Cell Growth, Phenocopying the Role of LIN28B

(A–D) Growth curves of control and neuroblastoma cell lines Kelly (A), NGP (B), SKNDZ (C), and SK-N-BE-2C (D) transfected with pooled RAN siRNAs. All cell lines are homozygous for the rs17065417 risk allele, which positively correlate with *LIN28B* expression (Diskin et al., 2012). In addition, NGP and SKNDZ exhibit regional 12q24 gain. Western blotting demonstrates knockdown of RAN, with Ku80 as loading control.

(E) Western blotting of LIN28B and RAN in NGP neuroblastoma cell lines with LIN28B depletion and RAN complementation.

(F) Cell proliferation in NGP neuroblastoma cell lines with LIN28B depletion and RAN complementation. Con, control. Error bars represent SEM. *$p < 0.01$ by Student's t test. **$p < 0.0001$.

See also Figure S2.

neuroblastomas. Collectively, our findings demonstrate that both LIN28B expression and chromosome 12q gain are associated with increased *RAN* mRNA expression, the former primarily in *MYCN* amplified cases, and the latter in high-risk tumors without *MYCN* amplification, and support the hypothesis that LIN28B and RAN can both drive a malignant phenotype in neuroblastoma.

RAN Promotes Neuroblastoma Cell Growth, Phenocopying the Effects of LIN28B

We and others showed that LIN28B depletion directly led to decreased neuroblastoma proliferation in vitro (Diskin et al., 2012; Molenaar et al., 2012a). To strengthen this observation, we demonstrated that LIN28B knockdown led to increased survival in a tail vein metastatic neuroblastoma model (Figure S2A). Although RAN positively regulates cell proliferation in multiple tumors, including pancreatic adenocarcinoma (Deng et al., 2013) and glioblastoma multiforme (Guvenc et al., 2013), its role in neuroblastoma was unknown. If one principal effect of LIN28B is to upregulate RAN expression, then RAN depletion would be expected to phenocopy LIN28B depletion. We first used pooled siRNAs to deplete RAN in neuroblastoma cell lines with high levels of *LIN28B* and *RAN*, demonstrating significant decreases in cellular proliferation, similar to what we and others previously observed with *LIN28B* depletion; Figures 2A–2D) Second, we depleted *RAN* with five independent shRNAs, demonstrating consequent decreases in cell proliferation (Figures S2B–S2D). Third, we overexpressed RAN in a neuroblastoma cell line with lower levels of RAN expression, demonstrating an increase in cell proliferation (Figure S2E). Finally, we determined whether RAN overexpression could rescue the decreased proliferation previously demonstrated with LIN28B knockdown (Diskin et al., 2012). We generated the following cell lines: (1) Control, (2) shLIN28B, (3) LIN28B depleted, with exogenous expression of RAN. Western blotting validated appropriate LIN28B and RAN expression (Figure 2E). With LIN28B knockdown, cell proliferation decreased and this effect was effectively rescued with restoration of RAN (Figure 2F), arguing that RAN is one of the important downstream effectors of LIN28B.

LIN28B Influences the Expression of RAN GTPase

We next focused on defining the mechanism by which LIN28B regulates RAN expression. We examined a subset of neuroblastoma cell lines (four with higher LIN28B levels and two with lower levels), confirming the positive correlation between LIN28B and RAN mRNA (Figure 3A) and protein (Figure 3B). Because RAN cycles between an activated and inactivated state, RAN-GTP and RAN-GDP, we investigated whether higher levels of total RAN correlated with higher levels of RAN-GTP. Cell lines with higher levels of LIN28B and total RAN (NGP and Kelly) had higher levels of RAN-GTP, compared to those with lower levels of LIN28B and total RAN (SK-N-SH and NB16; Figures 3C and S3A), suggesting that higher total RAN levels are associated with higher RAN-GTP levels. Because this assay does not quantify the amount of RAN-GDP, it does not distinguish between whether levels of RAN-GTP are increased relative to RAN-GDP or whether both RAN-GDP and RAN-GTP levels are similarly increased.

We next determined whether LIN28B directly influences RAN expression using both lentiviruses encoding an shRNA directed against LIN28B (shLIN28B-1) to deplete LIN28B in two neuroblastoma cell lines (Figures 3D and 3E) and an independent lentiviral shRNA pool (shLIN28B-p) to deplete LIN28B in a third neuroblastoma cell line (Figure 3F). We achieved effective LIN28B depletion, leading to decreased *RAN* mRNA and protein expression (Figures 3D–3F). To further define the effect of LIN28B on RAN expression, we depleted LIN28B using four additional shRNAs, again demonstrating that LIN28B knockdown led to

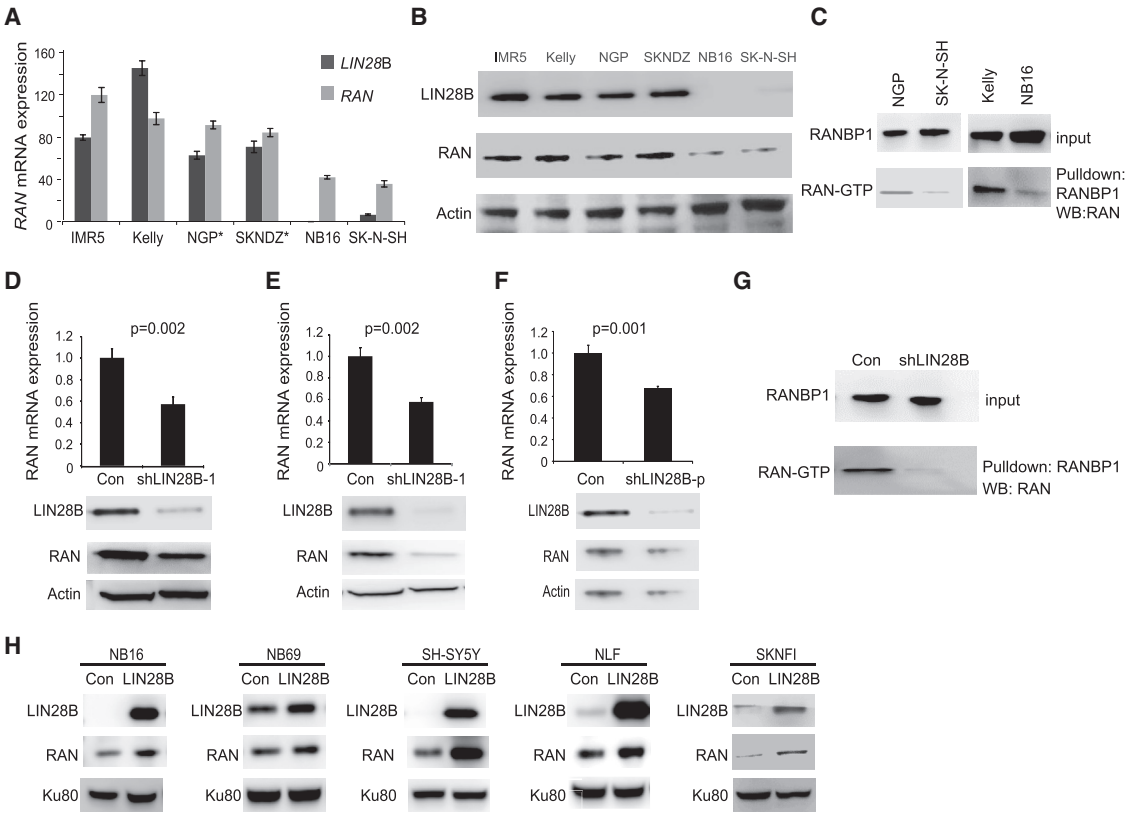

Figure 3. LIN28B Positively Influences the Expression of RAN GTPase

(A) Quantitative RT-PCR demonstrating *LIN28B* and *RAN* mRNA levels in neuroblastoma cell lines. Asterisk indicates cell lines with regional 12q24 gain.

(B) Immunoblotting analysis of LIN28B and RAN protein levels in neuroblastoma cell lines, with actin as loading control.

(C) RAN activation assay showing levels of RAN-GTP in NGP/SKNSH and Kelly/NB16 cell line pairs with high and low levels, respectively, of both LIN28B and RAN. Pulldowns were performed with RANBP1-bound agarose beads, followed by immunoblotting with anti-RAN antibody. RANBP1 immunoblot demonstrates equal loading in the input used for pulldown.

(D–F) RT-PCR demonstrating *RAN* mRNA levels in Kelly (D), NGP (E), and SKNDZ (F) neuroblastoma cell lines infected with lentiviruses encoding shRNAs directed against *LIN28B*. shLIN28B-p designates pooled shRNAs directed against *LIN28B*. *RAN* mRNA levels are normalized to *HPRT* levels and are shown relative to control. Immunoblots show expression of LIN28B and RAN, with actin as a loading control.

(G) RAN-GTP levels in the NGP cell line infected with control and shLIN28B-expressing lentiviruses. RANBP1 immunoblot demonstrates equal loading.

(H) Western blots for LIN28B and RAN expression in indicated cell lines infected with control and LIN28B-expressing lentiviruses, with Ku80 blots serving as loading controls. Error bars represent SEM, with p values listed in individual panels.

See also Figure S3.

RAN knockdown (Figures S3B and S3C). Moreover, LIN28B depletion decreased RAN-GTP levels (Figure 3G). To complement shRNA-mediated approaches, we expressed LIN28B in five neuroblastoma cell lines with lower levels of LIN28B protein and observed increases in RAN protein levels (Figure 3H). Collectively, these experiments argue that LIN28B promotes RAN expression.

LIN28B/let-7 Indirectly Regulates RAN Protein Levels via RAN Binding Protein 2

Because the most well-characterized function of LIN28B is its inhibition of let-7 microRNA maturation, we considered the possibility that RAN is a direct let-7 target. In both neuroblastoma cell lines and primary tumors, LIN28B and let-7 expression are inversely correlated (Diskin et al., 2012; Molenaar et al., 2012a) and depletion of LIN28B leads to increased levels of let-7 family members (Molenaar et al., 2012a), a finding that we further verified for let-7a and let-7i (Figure S4A). We transfected neuroblastoma cell lines with control and mature let-7a microRNA mimetics, bypassing the inhibitory effect of LIN28B on let-7 processing. Real-Time PCR verified significant let-7a overexpression (Figure 4A) and western blotting analysis demonstrated that let-7a expression led to a decrease in RAN levels and overexpression of let-7i similarly led to modest decreases in RAN expression (Figures 4B and S4B). We examined the microRNA target prediction databases Pictar (Krek et al., 2005), Targetscan (Lewis et al., 2005), and MicroRNA.org (Betel et al., 2008), but found no let-7 binding sites within RAN, arguing that RAN is not a canonical let-7 target. We speculated that let-7 might be indirectly influencing RAN expression, accounting for a more subtle effect on RAN levels with robust let-7 overexpression.

RANBP2, a protein that directly binds RAN (Melchior et al., 1995; Delphin et al., 1997; Yaseen and Blobel, 1999) and a component of the RAN signaling pathway that is correlated

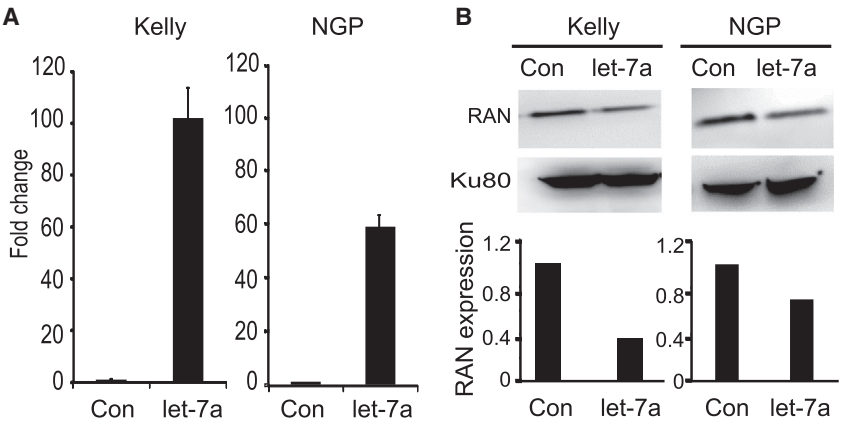

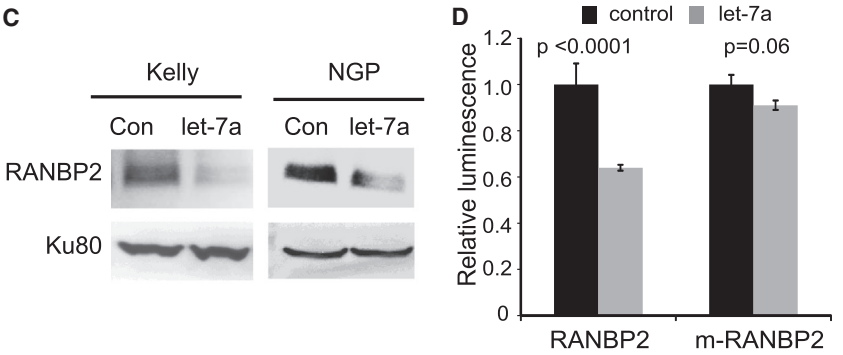

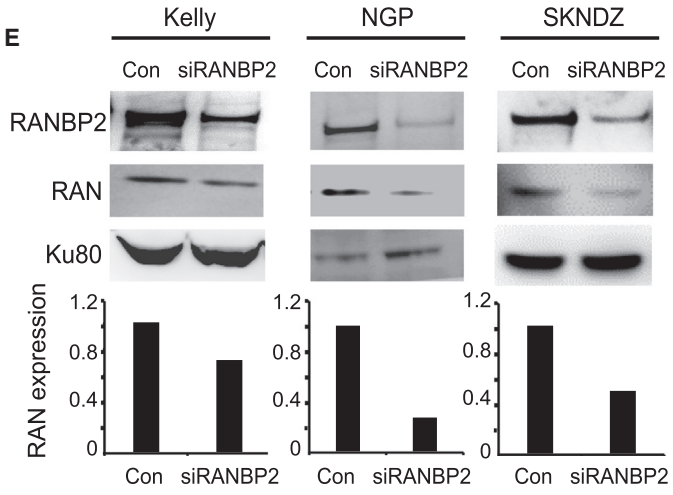

Figure 4. LIN28B/let-7 Indirectly Regulates RAN Protein Levels via RANBP2

(A) RT-PCR demonstrating expression of let-7a in Kelly and NGP neuroblastoma cell lines.

(B) Western blots demonstrating RAN protein expression in control and let-7 expressing cell lines, with Ku80 as loading control. ImageJ quantitation demonstrates relative RAN protein expression of 0.37 in Kelly and 0.70 in NGP.

(C) Western blots demonstrating RANBP2 protein expression in control and let-7 expressing cell lines, with Ku80 immunoblots as loading control.

(D) Control microRNA and mature let-7a were transfected into 293T cells and the effect on wild-type RANBP2 3′UTR and mutated RANBP2 (m-RANBP2) 3′UTR activity was quantitated.

(E) Western blots demonstrating RAN and RANBP2 protein expression in control and RANBP2 depleted cell lines (using pooled siRNAS) with Ku80 immunoblots as loading control. ImageJ quantitation demonstrates relative RAN protein expression of 0.71 in Kelly, 0.27 in NGP, and 0.49 in SKNDZ. Error bars represent SEM.

See also Figure S4.

with *LIN28B* expression (Table S3), emerged as a possible candidate mediating this influence, because it has two let-7 binding sites. Moreover, mice with conditional deletion of *Ranbp2* in their retinal pigmented epithelium develop retinal degeneration and, importantly, demonstrate lower levels of RAN protein but similar levels of *Ran* mRNA compared to wild-type mice, arguing that one function of RANBP2 is to stabilize RAN protein (Patil et al., 2014). Based on this finding, the presence of let-7 binding sites in RANBP2, and the binding of RANBP2 to RAN, we hypothesized that LIN28B/let-7 regulates RANBP2 expression, with RANBP2 in turn stabilizing RAN protein levels.

We showed that depletion of LIN28B led to decreased expression of RANBP2 (Figure S4C) and then evaluated the effect of let-7 on RANBP2 levels, finding that let-7a expression reduced RANBP2 protein levels (Figure 4C). We then demonstrated that RANBP2 is a direct let-7 target because treatment with let-7a inhibited RANBP2 3′UTR-driven luciferase activity (Figure 4D). Additionally, mutation of the let-7 binding sites in the RANBP2 3′UTR inhibited the ability of let-7 to decrease RANBP2 3′UTR-driven luciferase activity, indicating that LIN28B influences RANBP2 through let-7. If RANBP2 promotes the stability of RAN in neuroblastoma, as it does in the murine retina, then RANBP2 depletion should result in decreased RAN protein expression. Using pooled siRNAs directed against RANBP2, we depleted RANBP2 in three neuroblastoma cell lines, leading to reduction in RAN protein, quantified using ImageJ (Figure 4E). Taken together, these investigations suggest that LIN28B promotes RANBP2 expression in a let-7-dependent manner and that RANBP2 subsequently stabilizes the RAN protein.

RAN Is a Direct RNA Target of LIN28B

In addition to inhibiting let-7, LIN28A and LIN28B bind mRNAs directly, particularly at GGAG(A) and GAAG motifs and have been shown to promote translation of mRNAs to which they bind (Peng et al., 2011; Cho et al., 2012; Wilbert et al., 2012; Hafner et al., 2013; Madison et al., 2013). *RAN* contains 8 GGAGA

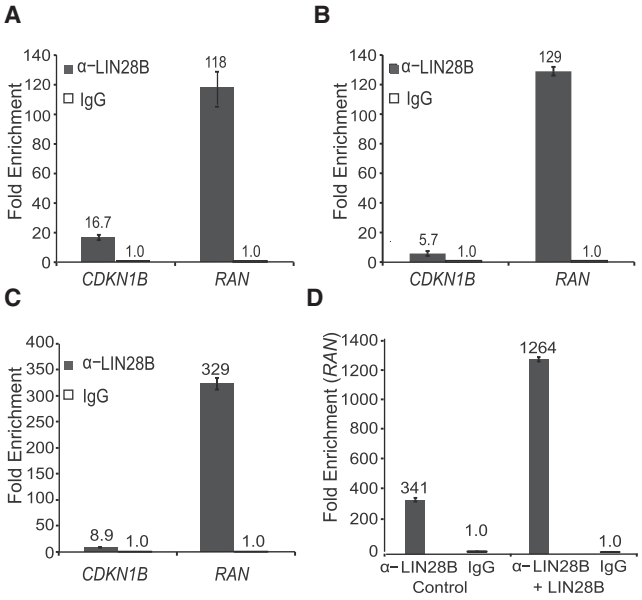

Figure 5. RAN Is a Direct RNA Target of LIN28B

(A–C) Quantitative RT-PCR analysis of *RAN* and *CDKN1B* mRNA levels in NGP (A), SKNDZ (B), and SK-N-BE-2C (C) lysates containing LIN28B-RNA complexes, immunoprecipitated with either anti- LIN28B antibody or control IgG. Fold enrichment is relative to RNA precipitated with control IgG. Results are representative of at least two independent experiments.

(D) Quantitative RT-PCR analysis of *RAN* mRNA levels in NB16 cell lines infected with control and LIN28B-expressing lentiviruses, normalized to *CDKN1B* binding. Results are representative of two independent experiments. Error bars represent SEM.

See also Figure S5.

and 13 GGAG motifs, which led us to speculate that LIN28B might directly bind *RAN* mRNA in neuroblastoma cells and to perform RNA-binding protein immunoprecipitation assays (RIP; (Keene et al., 2006) in neuroblastoma cell lines. We first immunoprecipitated RNA-protein complexes with control IgG and LIN28B antibody, along with antibodies directed against the RNA binding proteins EWSR1 and FXR1. Only RNA-protein complexes immunoprecipitated with LIN28B antibody (and not those immunoprecipitated with EWSR1 and FXR1 antibodies) were significantly enriched for *RAN*, arguing for the specificity of LIN28B binding to *RAN* mRNA (Figure S5A). We then immunoprecipitated RNA-protein complexes in three neuroblastoma cell lines and assayed LIN28B binding to *RAN* and to *CDKN1B*, an mRNA not enriched by binding to LIN28B in neuroblastoma cells. These studies (Figures 5A–5C) further demonstrated that LIN28B protein specifically binds *RAN* mRNA. To complement these approaches, we performed the RIP assay on two additional neuroblastoma cell lines, one with higher endogenous LIN28B and RAN levels (Kelly), and one with lower endogenous LIN28B and RAN levels (NB16; Figure S5B) and demonstrated that cell lines with higher levels of LIN28B were enriched for *RAN* binding. Finally, we examined the binding of LIN28B to *RAN* mRNA in the NB16 cell line overexpressing LIN28B (as shown in Figure 3H), demonstrating that cell lines engineered to express higher levels of LIN28B and RAN were enriched for *RAN* binding in comparison to control lines (Figure 5D). Collectively, these data demonstrate that LIN28B binds to *RAN* mRNA in neuroblastoma, possibly influencing RAN translation.

As additional evidence for the binding of LIN28B protein to *RAN* mRNA, we examined a ribonucleoprotein CLIP-Seq (cross-linking, immunoprecipitation, and high-throughput sequencing) dataset performed in human and murine colonic tissues and cell lines and found evidence for LIN28B binding to *RAN* mRNA in a colon cancer cell line (Madison et al., 2013). Together, these data demonstrate a direct link between LIN28B overexpression in neuroblastoma cells and enhanced RAN GTPase activity. Further investigation is required to delineate the exact mechanisms by which the binding of LIN28B to mRNAs influences the expression of RAN and other target genes.

LIN28B and RAN Signaling Converge on AURKA

We next investigated the signaling networks downstream of both LIN28B and RAN. RAN-GTP has been shown to induce phosphorylation of threonine 288 of AURKA (Tsai et al., 2003; Trieselmann et al., 2003), further increasing the enzymatic activity of AURKA and allowing it to promote cell cycle progression. Thus, we first confirmed that siRNA-mediated depletion of RAN led to decreased phosphorylation at threonine 288 of AURKA, with minimal changes in total levels of AURKA (Figure 6A), whereas overexpression of RAN led to an increase in phosphorylated AURKA (Figure S6A).

As LIN28B promotes the expression of RAN GTPase, we predicted that LIN28B depletion would decrease RAN protein expression, in turn decreasing phosphorylation at threonine 288. Surprisingly, pooled siRNA-mediated LIN28B knockdown reduced not only the levels of phosphorylated AURKA, but also total AURKA levels (Figure 6B). In addition, overexpression of LIN28B resulted in increased AURKA expression in five neuroblastoma cell lines (Figure S6B). We speculated that AURKA was a let-7 target and various microRNA target prediction programs (Krek et al., 2005; Lewis et al., 2005; Betel et al., 2008) predicted AURKA to have one let-7 binding site in its 3′UTR. Overexpression of let-7a phenocopied the effects of LIN28B depletion, reducing levels of both phosphorylated and total AURKA (Figure 6C). To verify that AURKA is a direct let-7 target, we performed 3′UTR reporter assays, showing that treatment with let-7a inhibited AURKA 3′UTR-driven luciferase activity (Figure 6D). Mutation of the let-7 binding site in the AURKA 3′UTR relieved the inhibitory effect of let-7a, arguing that AURKA is a direct let-7 target. Collectively, these experiments demonstrate that LIN28B indirectly influences AURKA by promoting RAN expression, and directly regulates AURKA through let-7.

In neuroblastoma, AURKA is being developed as a potential therapeutic target (Maris et al., 2010; Mosse et al., 2012) as AURKA has been shown to stabilize MYCN at the level of protein and shRNA-mediated depletion has been shown to lead to decreased cell proliferation in neuroblastoma (Otto et al., 2009; Cole et al., 2011). Consistent with these data, we found that depletion of AURKA reduced MYCN expression (Figure S6C). In further support of the link between LIN28B and AURKA signaling, expression of these two mRNAs is positively correlated in primary neuroblastomas (Valentijn et al., 2012; Oberthuer et al., 2010; Figures S6D–S6F) and high *AURKA* expression is associated with reduced overall survival (Figure S6G), as described (Otto et al., 2009).

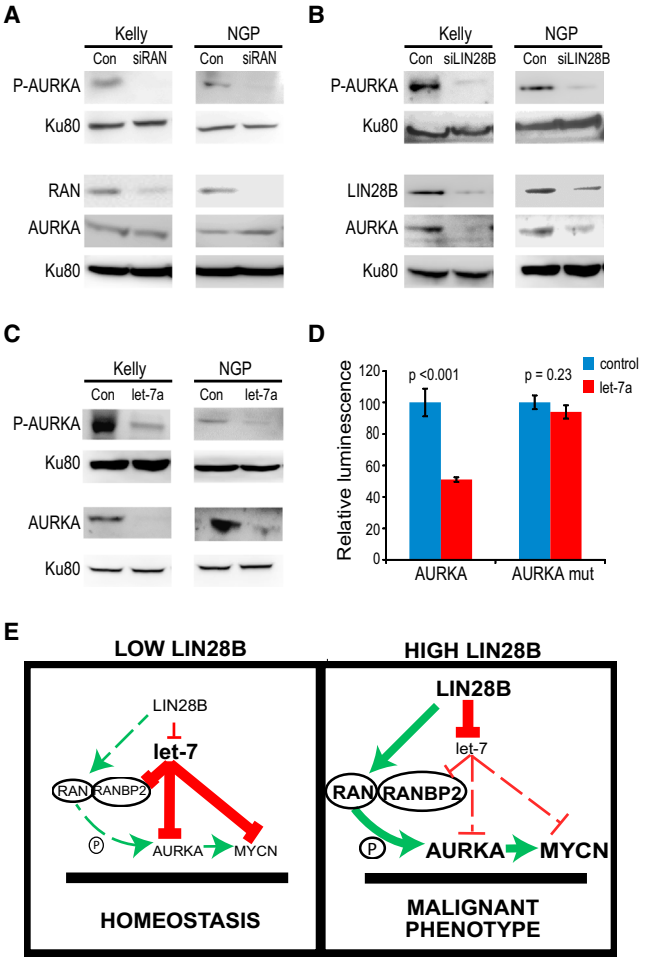

Figure 6. LIN28B and RAN Signaling Converge on AURKA

(A) Top images show immunoblots of AURKA phosphorylated at threonine 88 (designated P-AURKA) in control and RAN-depleted (with pooled siRNAs) cell lines, treated with nocodazole to enrich for G_2/M phase; Ku80 was used as the loading control. Bottom panels show Western blotting analysis of RAN and total AURKA in control and RAN-depleted cell lines, with Ku80 as the loading control.

(B) Top images show immunoblots of P-AURKA in control and LIN28B-depleted cell lines (using pooled siRNAs), treated with nocodazole. Bottom panels show Western blotting analysis of LIN28B, AURKA, and Ku80 in control and LIN28B-depleted Kelly and NGP cell lines.

(C) Top images show immunoblots of P-AURKA in control and let-7 expressing cell lines, treated with nocodazole. Bottom panels show western blotting analysis of AURKA and Ku80 in control and let-7 expressing cell lines.

(D) 3′UTR assays showing the effect of let-7 upon AURKA expression. Control microRNA and mature let-7a were transfected into 293T cells and the effect on wild-type AURKA 3′UTR and mutated AURKA 3′UTR activity was quantitated.

(E) Model depicting a proposed LIN28B-RAN-AURKA-MYCN signaling network and its role in driving neuroblastoma tumorigenesis. Error bars represent SEM.

See also Figure S6.

DISCUSSION

This work was motivated by the co-discovery of *LIN28B* as a neuroblastoma susceptibility gene (Diskin et al., 2012) and the demonstration that ectopic LIN28B expression in the developing murine sympathetic nervous system causes neuroblastoma, in part through enhancing MYCN expression (Molenaar et al., 2012a). We propose a central regulatory role for LIN28B in neuroblastoma, influencing both RAN and AURKA signaling.

We demonstrate RAN to be a key downstream component of LIN28B signaling, with RAN depletion decreasing cell proliferation and restoration of RAN levels helping to counter the decreased proliferation seen with LIN28B knockdown. In support of a broader oncogenic role, RAN, a member of the RAS superfamily of GTPases, is overexpressed in multiple malignancies, including pancreatic adenocarcinoma (Deng et al., 2013), glioblastoma multiforme (Guvenc et al., 2013), ovarian cancer (Barrès et al., 2010), and renal cell carcinoma (Abe et al., 2008). While the cycling between RAN-GTP and RAN-GDP clearly regulates RAN function, our work defines another mechanism influencing RAN levels, revealing that LIN28B increases RAN mRNA and protein levels. Similarly, mir-203 was shown to function as a tumor suppressor in esophageal cancer, in part via downregulating RAN mRNA and protein (Zhang et al., 2014). Highlighting the critical relationship between LIN28 and let-7, we demonstrate that RANBP2 is a let-7 target and show that RANBP2 helps stabilize RAN protein levels, though further investigation is needed to define how the RANBP2-RAN interaction promotes RAN stability. We also demonstrate that LIN28B directly binds *RAN* mRNA, illustrating a second mechanism by which LIN28B promotes RAN expression and consistent with previous reports showing that the LIN28 family binds mRNAs (Peng et al., 2011; Cho et al., 2012; Wilbert et al., 2012; Hafner et al., 2013; Madison et al., 2013).

The influence of LIN28B on RAN expression is most striking within *MYCN*-amplified tumors, consistent with our previous study identifying the correlation of *LIN28B* and *MYCN* expression (Diskin et al., 2012) and the observation that LIN28B directly promotes *MYCN* expression (Molenaar et al., 2012a). However, we also identify regional gain of chromosome 12q24 as an additional factor mediating increased *RAN* expression, most notably in the non-*MYCN* amplified subset of neuroblastoma, which generally expresses low levels of LIN28B. We speculate that, in the absence of higher levels of LIN28B expression, chromosome 12q24 regional gain might provide one alternate means of increasing *RAN* expression.

Our studies reveal a convergence of LIN28B and RAN signaling on AURKA. AURKA plays a crucial role in multiple malignancies, including neuroblastoma, where targeted inhibition is broadly cytotoxic (Maris, 2010). Whereas AURKA stabilizes the MYCN protein (Otto et al., 2009), the mechanisms for AURKA activation in neuroblastoma have not been previously defined. Our data suggest a possible mechanism for hyperactivation and thus identify a potential biomarker for drug sensitivity. In addition, Aurora kinase B has been implicated in neuroblastoma tumorigenesis (Morozova et al., 2010) and has been shown to be a let-7 target in germ cell tumors (Murray et al., 2013), but will require further investigation to establish a functional relationship with LIN28B expression.

These studies delineate a LIN28B-orchestrated signaling network (Figure 6E). LIN28B regulates RANBP2 levels and directly binds to *RAN* mRNA, providing indirect and direct mechanisms, respectively, of promoting RAN expression. Consistent with previous studies, RAN promotes the phosphorylation and activation of AURKA (Tsai et al., 2003; Trieselmann et al.,

2003). Additionally, LIN28B promotes AURKA expression directly via inhibition of let-7. AURKA serves as a point of convergence of LIN28B-RAN signaling, further driving cell cycle progression by phosphorylating a number of cell cycle regulators and stabilizing MYCN protein (Otto et al., 2009), which is itself a LIN28B/let-7 target (Molenaar et al., 2012a). This interplay among LIN28B, RAN, AURKA, and MYCN illustrates the complexity of LIN28B signaling in driving neuroblastoma tumorigenesis but also raises the possibility that combined targeting of these pathways may represent therapeutic opportunities in neuroblastoma. Although there are no direct RAN inhibitors, inhibitors directed against XPO1/CRM1, a protein that directly interacts with RAN to promote nuclear export and that is correlated with *LIN28B* expression, have shown efficacy against both liquid and solid malignancies (Nguyen et al., 2012). AURKA inhibitors have demonstrated therapeutic effect against solid tumors in preclinical modeling and are in Phase 2 trials in combination with chemotherapy for neuroblastoma (Mosse et al., 2012). Bromodomain and extraterminal (BET) inhibitors targeting the MYC family, including MYCN, have demonstrated efficacy in preclinical models of neuroblastoma (Puissant et al., 2013; Wyce et al., 2013), with clinical trials in development. Finally, let-7 has been proposed as a potential therapy in a number of cancers and was recently shown to reduce LIN28B-driven tumors in murine models of liver cancer (Nguyen et al., 2014). This work should allow investigators to develop responder hypotheses and possible drug combinations based on the biomarkers defined in this LIN28B-orchestrated signaling network.

EXPERIMENTAL PROCEDURES

Neuroblastoma Patient Datasets

All tumor and matched blood samples used in this study were from subjects enrolled on the Children's Oncology Group (COG) Neuroblastoma Biology Protocol ANBL00B1, with informed consent obtained by treating physicians at each COG institution. De-identified nucleic acids were shipped to the Children's Hospital of Philadelphia for study after COG and Cancer Therapy Evaluation Program (CTEP) scientific review and approval. The Children's Hospital of Philadelphia Institutional Review Board agreed with our determination that this research is considered exempt from the human subject research regulatory requirements in the Code of Federal Regulations. Further details regarding datasets are provided in the Supplemental Experimental Procedures.

The tumor genomics data are available through the Therapeutically Applicable Research to Generate Effective Treatments (TARGET) data matrix portal (http://target.nci.nih.gov/dataMatrix/TARGET_DataMatrix.html).

Cell Culture

Neuroblastoma cell lines were passaged in RPMI-containing media; 293T cells were grown in DMEM supplemented similarly. To enrich for cells in G_2/M, Kelly, NGP, and NB16 cells were treated with 100, 200, and 300 ng/ml nocodazole, respectively, for 24 hr.

Real-Time PCR Analysis

Experiments were performed with standard methodology and are detailed in the Supplemental Experimental Procedures.

Western Blotting

Immunoblotting was performed with standard methods, further detailed in the Supplemental Experimental Procedures.

RAN Activation Assays

Assays were performed using the RAN Activation Assay kit (Cell Biolabs). Briefly, 750 μg of lysates was incubated for one hour at 4°C with agarose beads conjugated to RANBP1, which specifically binds RAN-GTP and not RAN-GDP. Beads were pelleted, washed, and resuspended in SDS-PAGE buffer, followed by immunoblotting with an anti-RAN antibody.

Lentiviral Preparation and Transduction

Lentiviral preparation was carried out as described (Liu et al., 2013) and further outlined in the Supplemental Experimental Procedures.

RNA Immunoprecipitation Assays

RNA immunoprecipitation assays were performed using the MagnaRIP RNA Binding Protein Immunoprecipitation kit (Millipore). RNA levels were quantified by RT-PCR.

3′UTR Luciferase Reporter Assays

Assays were conducted on 293T cells using the Lightswitch Luciferase Assay System (Switchgear Genomics). Briefly, cells were transfected, incubated for 24 hr, and then harvested for luciferase assays as per the manufacturer's instructions. Further experimental details are outlined in the Supplemental Experimental Procedures.

Cell Proliferation Assays

To determine the effect of transient RAN knockdown on cell proliferation, the RT-CES system, as described (Diskin et al., 2012), was used, and cell viability was measured using CellTiter-Glo Cell viability assays (Promega) following the manufacturer's protocol, with further details described in the Supplemental Experimental Procedures.

Statistical Analyses

Statistical analyses were performed using Microsoft Excel and the R programming language, unpaired Student's t test. Statistical methodology for gene expression profiling and GISTIC analyses is described in the Supplemental Experimental Procedures. ImageJ software was used for quantitation of select immunoblots.

SUPPLEMENTAL INFORMATION

Supplemental Information includes Supplemental Experimental Procedures, six figures, and five tables and can be found with this article online at http://dx.doi.org/10.1016/j.ccell.2015.09.012.

AUTHOR CONTRIBUTIONS

R.W.S., J.M.M., and S.J.D. designed the experiments and drafted the manuscript. S.J.D. analyzed mRNA expression data and performed Ingenuity analysis. S.J.D., E.F.A., and P.R. analyzed copy-number data and performed GISTIC analysis. R.W.S., P.K., S.E.C., M.E.G., and K.L.C. generated cell lines and performed RT-PCR analysis, Western blotting, and cell proliferation assays. R.S. and P.K. performed GTPase assays, RIP assays, and 3′UTR luciferase assays. D.A.O. analyzed LIN28B binding sites in *RAN* mRNA and P.R. performed Kaplan-Meier analyses. B.B.M. and A.K.R. shared CLIP-Seq data and S.A. and R.C.S. participated in the generation of the TARGET neuroblastoma dataset. All authors commented on or contributed to the current manuscript.

ACKNOWLEDGMENTS

This work was supported in part by NIH grants R01-CA124709 (to J.M.M.), 1RC1MD004418-01 (to J.M.M), R00-CA151869 (to S.J.D.), T32 CA009615 (to R.W.S.), K12 HD04324 (to R.W.S.), the Giulio D'Angio Endowed Chair (to J.M.M.), the Alex's Lemonade Stand Foundation (to R.W.S. and J.M.M.), Andrew's Army Foundation (to J.M.M.), the Abramson Family Cancer Research Institute (to J.M.M.), K01 DK093885 (to B.B.M.), and R01-DK 056645 (to B.B.M. and A.K.R.).

Received: February 14, 2015
Revised: June 18, 2015
Accepted: September 22, 2015
Published: October 15, 2015

REFERENCES

Abe, H., Kamai, T., Shirataki, H., Oyama, T., Arai, K., and Yoshida, K. (2008). High expression of Ran GTPase is associated with local invasion and metastasis of human clear cell renal cell carcinoma. Int. J. Cancer *122*, 2391–2397.

Barrès, V., Ouellet, V., Lafontaine, J., Tonin, P.N., Provencher, D.M., and Mes-Masson, A.M. (2010). An essential role for Ran GTPase in epithelial ovarian cancer cell survival. Mol. Cancer *9*, 272.

Beroukhim, R., Getz, G., Nghiemphu, L., Barretina, J., Hsueh, T., Linhart, D., Vivanco, I., Lee, J.C., Huang, J.H., Alexander, S., et al. (2007). Assessing the significance of chromosomal aberrations in cancer: methodology and application to glioma. Proc. Natl. Acad. Sci. USA *104*, 20007–20012.

Betel, D., Wilson, M., Gabow, A., Marks, D.S., and Sander, C. (2008). The microRNA.org resource: targets and expression. Nucleic Acids Res. *36*, D149–D153.

Bosse, K.R., Diskin, S.J., Cole, K.A., Wood, A.C., Schnepp, R.W., Norris, G., Nguyen, B., Jagannathan, J., Laquaglia, M., Winter, C., et al. (2012). Common variation at BARD1 results in the expression of an oncogenic isoform that influences neuroblastoma susceptibility and oncogenicity. Cancer Res. *72*, 2068–2078.

Boyerinas, B., Park, S.M., Hau, A., Murmann, A.E., and Peter, M.E. (2010). The role of let-7 in cell differentiation and cancer. Endocr. Relat. Cancer *17*, F19–F36.

Bresler, S.C., Weiser, D.A., Huwe, P.J., Park, J.H., Krytska, K., Ryles, H., Laudenslager, M., Rappaport, E.F., Wood, A.C., McGrady, P.W., et al. (2014). ALK mutations confer differential oncogenic activation and sensitivity to ALK inhibition therapy in neuroblastoma. Cancer Cell *26*, 682–694.

Capasso, M., Devoto, M., Hou, C., Asgharzadeh, S., Glessner, J.T., Attiyeh, E.F., Mosse, Y.P., Kim, C., Diskin, S.J., Cole, K.A., et al. (2009). Common variations in BARD1 influence susceptibility to high-risk neuroblastoma. Nat. Genet. *41*, 718–723.

Cheung, N.K., Zhang, J., Lu, C., Parker, M., Bahrami, A., Tickoo, S.K., Heguy, A., Pappo, A.S., Federico, S., Dalton, J., et al. (2012). Association of age at diagnosis and genetic mutations in patients with neuroblastoma. JAMA. *307*, 1062–1071.

Cho, J., Chang, H., Kwon, S.C., Kim, B., Kim, Y., Choe, J., Ha, M., Kim, Y.K., and Kim, V.N. (2012). LIN28A is a suppressor of ER-associated translation in embryonic stem cells. Cell *151*, 765–777.

Clarke, P.R., and Zhang, C. (2008). Spatial and temporal coordination of mitosis by Ran GTPase. Nat. Rev. Mol. Cell Biol. *9*, 464–477.

Cole, K.A., Huggins, J., Laquaglia, M., Hulderman, C.E., Russell, M.R., Bosse, K., Diskin, S.J., Attiyeh, E.F., Sennett, R., Norris, G., et al. (2011). RNAi screen of the protein kinome identifies checkpoint kinase 1 (CHK1) as a therapeutic target in neuroblastoma. Proc. Natl. Acad. Sci. USA *108*, 3336–3341.

Delphin, C., Guan, T., Melchior, F., and Gerace, L. (1997). RanGTP targets p97 to RanBP2, a filamentous protein localized at the cytoplasmic periphery of the nuclear pore complex. Mol. Biol. Cell *8*, 2379–2390.

Deng, L., Lu, Y., Zhao, X., Sun, Y., Shi, Y., Fan, H., Liu, C., Zhou, J., Nie, Y., Wu, K., et al. (2013). Ran GTPase protein promotes human pancreatic cancer proliferation by deregulating the expression of Survivin and cell cycle proteins. Biochem. Biophys. Res. Commun. *440*, 322–329.

Diskin, S.J., Capasso, M., Schnepp, R.W., Cole, K.A., Attiyeh, E.F., Hou, C., Diamond, M., Carpenter, E.L., Winter, C., Lee, H., et al. (2012). Common variation at 6q16 within HACE1 and LIN28B influences susceptibility to neuroblastoma. Nat. Genet. *44*, 1126–1130.

Esquela-Kerscher, A., Trang, P., Wiggins, J.F., Patrawala, L., Cheng, A., Ford, L., Weidhaas, J.B., Brown, D., Bader, A.G., and Slack, F.J. (2008). The let-7 microRNA reduces tumor growth in mouse models of lung cancer. Cell Cycle *7*, 759–764.

Guvenc, H., Pavlyukov, M.S., Joshi, K., Kurt, H., Banasavadi-Siddegowda, Y.K., Mao, P., Hong, C., Yamada, R., Kwon, C.H., Bhasin, D., et al. (2013). Impairment of glioma stem cell survival and growth by a novel inhibitor for Survivin-Ran protein complex. Clin. Cancer Res. *19*, 631–642.

Hafner, M., Max, K.E., Bandaru, P., Morozov, P., Gerstberger, S., Brown, M., Molina, H., and Tuschl, T. (2013). Identification of mRNAs bound and regulated by human LIN28 proteins and molecular requirements for RNA recognition. RNA *19*, 613–626.

Helland, Å., Anglesio, M.S., George, J., Cowin, P.A., Johnstone, C.N., House, C.M., Sheppard, K.E., Etemadmoghadam, D., Melnyk, N., Rustgi, A.K., et al.; Australian Ovarian Cancer Study Group (2011). Deregulation of MYCN, LIN28B and LET7 in a molecular subtype of aggressive high-grade serous ovarian cancers. PLoS ONE *6*, e18064.

Keene, J.D., Komisarow, J.M., and Friedersdorf, M.B. (2006). RIP-Chip: the isolation and identification of mRNAs, microRNAs and protein components of ribonucleoprotein complexes from cell extracts. Nat. Protoc. *1*, 302–307.

King, C.E., Cuatrecasas, M., Castells, A., Sepulveda, A.R., Lee, J.S., and Rustgi, A.K. (2011a). LIN28B promotes colon cancer progression and metastasis. Cancer Res. *71*, 4260–4268.

King, C.E., Wang, L., Winograd, R., Madison, B.B., Mongroo, P.S., Johnstone, C.N., and Rustgi, A.K. (2011b). LIN28B fosters colon cancer migration, invasion and transformation through let-7-dependent and -independent mechanisms. Oncogene *30*, 4185–4193.

Krek, A., Grün, D., Poy, M.N., Wolf, R., Rosenberg, L., Epstein, E.J., MacMenamin, P., da Piedade, I., Gunsalus, K.C., Stoffel, M., and Rajewsky, N. (2005). Combinatorial microRNA target predictions. Nat. Genet. *37*, 495–500.

Lewis, B.P., Burge, C.B., and Bartel, D.P. (2005). Conserved seed pairing, often flanked by adenosines, indicates that thousands of human genes are microRNA targets. Cell *120*, 15–20.

Liu, F., Zhang, X., Weisberg, E., Chen, S., Hur, W., Wu, H., Zhao, Z., Wang, W., Mao, M., Cai, C., et al. (2013). Discovery of a selective irreversible BMX inhibitor for prostate cancer. ACS Chem. Biol. *8*, 1423–1428.

Madison, B.B., Liu, Q., Zhong, X., Hahn, C.M., Lin, N., Emmett, M.J., Stanger, B.Z., Lee, J.S., and Rustgi, A.K. (2013). LIN28B promotes growth and tumorigenesis of the intestinal epithelium via Let-7. Genes Dev. *27*, 2233–2245.

Maris, J.M. (2010). Recent advances in neuroblastoma. N. Engl. J. Med. *362*, 2202–2211.

Maris, J.M., Morton, C.L., Gorlick, R., Kolb, E.A., Lock, R., Carol, H., Keir, S.T., Reynolds, C.P., Kang, M.H., Wu, J., et al. (2010). Initial testing of the aurora kinase A inhibitor MLN8237 by the Pediatric Preclinical Testing Program (PPTP). Pediatr. Blood Cancer *55*, 26–34.

Melchior, F., Guan, T., Yokoyama, N., Nishimoto, T., and Gerace, L. (1995). GTP hydrolysis by Ran occurs at the nuclear pore complex in an early step of protein import. J. Cell Biol. *131*, 571–581.

Molenaar, J.J., Domingo-Fernández, R., Ebus, M.E., Lindner, S., Koster, J., Drabek, K., Mestdagh, P., van Sluis, P., Valentijn, L.J., van Nes, J., et al. (2012a). LIN28B induces neuroblastoma and enhances MYCN levels via let-7 suppression. Nat. Genet. *44*, 1199–1206.

Molenaar, J.J., Koster, J., Zwijnenburg, D.A., van Sluis, P., Valentijn, L.J., van der Ploeg, I., Hamdi, M., van Nes, J., Westerman, B.A., van Arkel, J., et al. (2012b). Sequencing of neuroblastoma identifies chromothripsis and defects in neuritogenesis genes. Nature *483*, 589–593.

Morozova, O., Vojvodic, M., Grinshtein, N., Hansford, L.M., Blakely, K.M., Maslova, A., Hirst, M., Cezard, T., Morin, R.D., Moore, R., et al. (2010). System-level analysis of neuroblastoma tumor-initiating cells implicates AURKB as a novel drug target for neuroblastoma. Clin. Cancer Res. *16*, 4572–4582.

Mosse, Y.P., Lipsitz, E., Fox, E., Teachey, D.T., Maris, J.M., Weigel, B., Adamson, P.C., Ingle, M.A., Ahern, C.H., and Blaney, S.M. (2012). Pediatric phase I trial and pharmacokinetic study of MLN8237, an investigational oral selective small-molecule inhibitor of Aurora kinase A: a Children's Oncology Group Phase I Consortium study. Clin. Cancer Res. *18*, 6058–6064.

Murray, M.J., Saini, H.K., Siegler, C.A., Hanning, J.E., Barker, E.M., van Dongen, S., Ward, D.M., Raby, K.L., Groves, I.J., Scarpini, C.G., et al.; CCLG (2013). LIN28 Expression in malignant germ cell tumors downregulates let-7 and increases oncogene levels. Cancer Res. *73*, 4872–4884.

Nguyen, K.T., Holloway, M.P., and Altura, R.A. (2012). The CRM1 nuclear export protein in normal development and disease. Int. J. Biochem. Mol. Biol. *3*, 137–151.

Nguyen, L.H., Robinton, D.A., Seligson, M.T., Wu, L., Li, L., Rakheja, D., Comerford, S.A., Ramezani, S., Sun, X., Parikh, M.S., et al. (2014). Lin28b is sufficient to drive liver cancer and necessary for its maintenance in murine models. Cancer Cell *26*, 248–261.

Oberthuer, A., Hero, B., Berthold, F., Juraeva, D., Faldum, A., Kahlert, Y., Asgharzadeh, S., Seeger, R., Scaruffi, P., Tonini, G.P., et al. (2010). Prognostic impact of gene expression-based classification for neuroblastoma. J. Clin. Oncol. *28*, 3506–3515.

Oh, J.S., Kim, J.J., Byun, J.Y., and Kim, I.A. (2010). Lin28-let7 modulates radiosensitivity of human cancer cells with activation of K-Ras. Int. J. Radiat. Oncol. Biol. Phys. *76*, 5–8.

Otto, T., Horn, S., Brockmann, M., Eilers, U., Schüttrumpf, L., Popov, N., Kenney, A.M., Schulte, J.H., Beijersbergen, R., Christiansen, H., et al. (2009). Stabilization of N-Myc is a critical function of Aurora A in human neuroblastoma. Cancer Cell *15*, 67–78.

Park, S.M., Shell, S., Radjabi, A.R., Schickel, R., Feig, C., Boyerinas, B., Dinulescu, D.M., Lengyel, E., and Peter, M.E. (2007). Let-7 prevents early cancer progression by suppressing expression of the embryonic gene HMGA2. Cell Cycle *6*, 2585–2590.

Patil, H., Saha, A., Senda, E., Cho, K.I., Haque, M., Yu, M., Qiu, S., Yoon, D., Hao, Y., Peachey, N.S., and Ferreira, P.A. (2014). Selective impairment of a subset of Ran-GTP-binding domains of ran-binding protein 2 (Ranbp2) suffices to recapitulate the degeneration of the retinal pigment epithelium (RPE) triggered by Ranbp2 ablation. J. Biol. Chem. *289*, 29767–29789.

Peng, S., Chen, L.L., Lei, X.X., Yang, L., Lin, H., Carmichael, G.G., and Huang, Y. (2011). Genome-wide studies reveal that Lin28 enhances the translation of genes important for growth and survival of human embryonic stem cells. Stem Cells *29*, 496–504.

Piskounova, E., Polytarchou, C., Thornton, J.E., LaPierre, R.J., Pothoulakis, C., Hagan, J.P., Iliopoulos, D., and Gregory, R.I. (2011). Lin28A and Lin28B inhibit let-7 microRNA biogenesis by distinct mechanisms. Cell *147*, 1066–1079.

Pugh, T.J., Morozova, O., Attiyeh, E.F., Asgharzadeh, S., Wei, J.S., Auclair, D., Carter, S.L., Cibulskis, K., Hanna, M., Kiezun, A., et al. (2013). The genetic landscape of high-risk neuroblastoma. Nat. Genet. *45*, 279–284.

Puissant, A., Frumm, S.M., Alexe, G., Bassil, C.F., Qi, J., Chanthery, Y.H., Nekritz, E.A., Zeid, R., Gustafson, W.C., Greninger, P., et al. (2013). Targeting MYCN in neuroblastoma by BET bromodomain inhibition. Cancer Discov. *3*, 308–323.

Sampson, V.B., Rong, N.H., Han, J., Yang, Q., Aris, V., Soteropoulos, P., Petrelli, N.J., Dunn, S.P., and Krueger, L.J. (2007). MicroRNA let-7a down-regulates MYC and reverts MYC-induced growth in Burkitt lymphoma cells. Cancer Res. *67*, 9762–9770.

Sausen, M., Leary, R.J., Jones, S., Wu, J., Reynolds, C.P., Liu, X., Blackford, A., Parmigiani, G., Diaz, L.A., Jr., Papadopoulos, N., et al. (2013). Integrated genomic analyses identify ARID1A and ARID1B alterations in the childhood cancer neuroblastoma. Nat. Genet. *45*, 12–17.

Shyh-Chang, N., Zhu, H., Yvanka de Soysa, T., Shinoda, G., Seligson, M.T., Tsanov, K.M., Nguyen, L., Asara, J.M., Cantley, L.C., and Daley, G.Q. (2013). Lin28 enhances tissue repair by reprogramming cellular metabolism. Cell *155*, 778–792.

Trieselmann, N., Armstrong, S., Rauw, J., and Wilde, A. (2003). Ran modulates spindle assembly by regulating a subset of TPX2 and Kid activities including Aurora A activation. J. Cell Sci. *116*, 4791–4798.

Tsai, M.Y., Wiese, C., Cao, K., Martin, O., Donovan, P., Ruderman, J., Prigent, C., and Zheng, Y. (2003). A Ran signalling pathway mediated by the mitotic kinase Aurora A in spindle assembly. Nat. Cell Biol. *5*, 242–248.

Urbach, A., Yermalovich, A., Zhang, J., Spina, C.S., Zhu, H., Perez-Atayde, A.R., Shukrun, R., Charlton, J., Sebire, N., Mifsud, W., et al. (2014). Lin28 sustains early renal progenitors and induces Wilms tumor. Genes Dev. *28*, 971–982.

Valentijn, L.J., Koster, J., Haneveld, F., Aissa, R.A., van Sluis, P., Broekmans, M.E., Molenaar, J.J., van Nes, J., and Versteeg, R. (2012). Functional MYCN signature predicts outcome of neuroblastoma irrespective of MYCN amplification. Proc. Natl. Acad. Sci. USA *109*, 19190–19195.

Viswanathan, S.R., Daley, G.Q., and Gregory, R.I. (2008). Selective blockade of microRNA processing by Lin28. Science *320*, 97–100.

Viswanathan, S.R., Powers, J.T., Einhorn, W., Hoshida, Y., Ng, T.L., Toffanin, S., O'Sullivan, M., Lu, J., Phillips, L.A., Lockhart, V.L., et al. (2009). Lin28 promotes transformation and is associated with advanced human malignancies. Nat. Genet. *41*, 843–848.

Wang, Q., Diskin, S., Rappaport, E., Attiyeh, E., Mosse, Y., Shue, D., Seiser, E., Jagannathan, J., Shusterman, S., Bansal, M., et al. (2006). Integrative genomics identifies distinct molecular classes of neuroblastoma and shows that multiple genes are targeted by regional alterations in DNA copy number. Cancer Res. *66*, 6050–6062.

Wang, Y.C., Chen, Y.L., Yuan, R.H., Pan, H.W., Yang, W.C., Hsu, H.C., and Jeng, Y.M. (2010). Lin-28B expression promotes transformation and invasion in human hepatocellular carcinoma. Carcinogenesis *31*, 1516–1522.

Wang, K., Diskin, S.J., Zhang, H., Attiyeh, E.F., Winter, C., Hou, C., Schnepp, R.W., Diamond, M., Bosse, K., Mayes, P.A., et al. (2011). Integrative genomics identifies LMO1 as a neuroblastoma oncogene. Nature *469*, 216–220.

Wang, L., Yuan, C., Lv, K., Xie, S., Fu, P., Liu, X., Chen, Y., Qin, C., Deng, W., and Hu, W. (2013). Lin28 mediates radiation resistance of breast cancer cells via regulation of caspase, H2A.X and Let-7 signaling. PLoS ONE *8*, e67373.

Wilbert, M.L., Huelga, S.C., Kapeli, K., Stark, T.J., Liang, T.Y., Chen, S.X., Yan, B.Y., Nathanson, J.L., Hutt, K.R., Lovci, M.T., et al. (2012). LIN28 binds messenger RNAs at GGAGA motifs and regulates splicing factor abundance. Mol. Cell *48*, 195–206.

Wolf, M., Korja, M., Karhu, R., Edgren, H., Kilpinen, S., Ojala, K., Mousses, S., Kallioniemi, A., and Haapasalo, H. (2010). Array-based gene expression, CGH and tissue data defines a 12q24 gain in neuroblastic tumors with prognostic implication. BMC Cancer *10*, 181.

Wyce, A., Ganji, G., Smitheman, K.N., Chung, C.W., Korenchuk, S., Bai, Y., Barbash, O., Le, B., Craggs, P.D., McCabe, M.T., et al. (2013). BET inhibition silences expression of MYCN and BCL2 and induces cytotoxicity in neuroblastoma tumor models. PLoS ONE *8*, e72967.

Xia, F., Lee, C.W., and Altieri, D.C. (2008). Tumor cell dependence on Ran-GTP-directed mitosis. Cancer Res. *68*, 1826–1833.

Yaseen, N.R., and Blobel, G. (1999). Two distinct classes of Ran-binding sites on the nucleoporin Nup-358. Proc. Natl. Acad. Sci. USA *96*, 5516–5521.

Yu, J., Vodyanik, M.A., Smuga-Otto, K., Antosiewicz-Bourget, J., Frane, J.L., Tian, S., Nie, J., Jonsdottir, G.A., Ruotti, V., Stewart, R., et al. (2007). Induced pluripotent stem cell lines derived from human somatic cells. Science *318*, 1917–1920.

Zhang, F., Yang, Z., Cao, M., Xu, Y., Li, J., Chen, X., Gao, Z., Xin, J., Zhou, S., Zhou, Z., et al. (2014). MiR-203 suppresses tumor growth and invasion and down-regulates MiR-21 expression through repressing Ran in esophageal cancer. Cancer Lett. *342*, 121–129.

Zhu, H., Shyh-Chang, N., Segrè, A.V., Shinoda, G., Shah, S.P., Einhorn, W.S., Takeuchi, A., Engreitz, J.M., Hagan, J.P., Kharas, M.G., et al.; DIAGRAM Consortium; MAGIC Investigators (2011). The Lin28/let-7 axis regulates glucose metabolism. Cell *147*, 81–94.